Asynchronous Switched Event-Triggered Load Frequency Control in Multi-Area Power Systems with Stochastic Actuator Failures

Yajian Zhang, Jiafang Zhang, Chen Peng and Fei Xue

August 4, 2023

Asynchronous Switched Event-Triggered Load Frequency Control in Multi-area Power Systems With Stochastic Actuator Failures

Yajian Zhang
School of Mechatronic Engineering and Automation
Shanghai University
Shanghai, China
zhang_ya_jian@shu.edu.cn

Jiafang Zhang
School of Mechatronic Engineering and Automation
Shanghai University
Shanghai, China
jiafangzhang@shu.edu.cn

Chen Peng*
School of Mechatronic Engineering and Automation
Shanghai University
Shanghai, China
c.peng@i.shu.edu.cn

Fei Xue
Institute of Power Science Research
Ningxia Electric Power Company
Ningxia, China
tjuxf1010@126.com

***Abstract*—Stochastic actuator failures caused by such as spring aging or hydraulic leakage may result in random switches among different operating modes of the load frequency control (LFC) system, posing a serious challenge to the frequency stability of multi-area power systems. Thereby, an asynchronous switched adaptive event-triggered LFC strategy is investigated in this paper. A series of operating scenarios are firstly preset according to the actuator failure severities. Then the event-triggered control (ETC) parameters containing controller and event-triggered detector (ETD) which corresponds to each faulty scenario are designed to stabilize the LFC system with a low network bandwidth occupancy. Fully considering that the controller and ETD cannot be simultaneously adjusted due to the existence of communication network, design constraints and update criteria of ETC parameters are strictly derived to guarantee exponential stability when the LFC system switches among different faulty scenarios. Finally, the effectiveness of the proposed method has been verified by conducting a series of simulations.**

***Index Terms*—load frequency control, event-triggered control, asynchronous switched control, actuator failure, multi-area power system**

I. Introduction

CONTINUOUS frequency deviations and tie-line power fluctuations caused by active power supply-and-demand imbalances have adverse effects on the safe and economic operations of multi-area power systems. Hence, the load frequency control (LFC) mechanism which adjusts the active power outputs of generators to re-balance active power supplies and load demands at rated frequency point is usually adopted by the control center [1]. However, the generators, as the actuating devices, may fail to respond to the required active power output instructions from the control center due to the sudden physical failures [2]. More seriously, persistent tie-line power oscillations or even separation accidents may occurs [3]. Different from the obvious failures such as blade fracture or valve blockage, stochastic latent failures such as insulation aging and loose contact may cause the generators cannot always keep the normal operating statuses.

Another trend in LFC is that the control center has increasingly relied on the communication network to transmit operating statuses and control instructions due to the complexity and scale expansions [4]. In traditional periodic-triggered LFC schemes [5], communication demands at each sampling instant are always required. To reduce the competitions for limited network resources in real-time applications (e.g., LFC, automatic voltage control [6], event-triggered control (ETC) schemes have been proposed [7]. Design constraints for ETD and controller have been presented by Peng et al [8]. However, triggered thresholds in aforementioned ETC schemes keep fixed, which means there is still a redundant data transmission when the state deviations have been well damped. Therefore, an adaptive event-triggered LFC scheme has been proposed in [9], where the triggered threshold is designed to be adaptively increased with the decrease of system state deviations.More works about adaptive event-triggered LFC can be found in [10]. However, most existing threshold adjustment schemes adopt an exponential update mechanism without any upper bound restrictions. It means that the triggered threshold will be quickly increased when system deviations start to be damped, resulting a long recovery time of grid frequency or continuous tie-line power oscillations.

Under actuator failure scenarios, frequency deviations may be difficult to be damped to zero since the generators cannot exactly output the active power required by the control center. Thereby, communications between control center and power plants may be frequently requested in the event-triggered LFC system without considering the faulty scenarios during design process. Shen et al [11] have described the actuator failure as a "0-1" switched model and then designed a H_∞ event-triggered

This work was supported in part by the National Natural Science Foundation of China under Grants 62173218, 61833011, and 62103254; and in part by the International Corporation Project of Shanghai Science and Technology Commission under Grant 21190780300. (Corresponding author: Chen Peng)

Y. Zhang, C. Peng, and M. Zheng are with the School of Mechatronic Engineering and Automation, and Shanghai Key Laboratory of Power Station Automation Technology, Shanghai University, Shanghai 200444, China (e-mail: c.peng@shu.edu.cn).

T. Yang are with the School of Electrical Automation and Information Engineering, Tianjin University, Tianjin, 300072, China (e-mail: yangtting@tju.edu.cn).

LFC scheme. The maximal tolerant transmission delay bound under actuator failures has been calculated. However, only one fixed controller is designed to simultaneously stabilize the normal and faulty scenarios, which has the disadvantages as many design constraints and strong conservatism. Similarly, simply describing the stochastic actuator failures as the parameter uncertainties also has the above shortcomings.

Actually, similar to the active fault tolerant control (AFTC) schemes in existing literature [12], if the controller gain is adaptively adjusted according to the failure scenarios, the control flexibility of LFC system can be effectively improved with less design conservatism. However, designing an adaptive ETC scheme with variable controller gain and ETD is very challenging. The reason is that ETD and controller are on opposite sides of the communication network, and the parameters of these two modules cannot be adjusted simultaneously when the actuator failure scenario changes [13]. Therefore, an asynchronous switched event-triggered LFC scheme is investigated in this paper. Main contributions are as follows.

(1) A series of actuator failure scenarios representing different severities is firstly preset. Compared with current event-triggered LFC schemes [8]- [11], the ETC parameters containing controller and ETD are adaptively adjusted according to the actuator failure scenarios. In addition, different from current ETC schemes adopting an unbounded threshold update mechanism [9]- [10], the threshold in this paper is restricted within a specific range to guarantee a sensitive awareness ability to the operating statuses of LFC system.

(2) Fully considering that the controller and ETD are located on the opposite sides of the communication network, the update process of the two modules in arbitrary two faulty switching case are characterized as a asynchronous switching model. Design constraints and the corresponding update criteria are strictly derived by constructing the Lyapunov functions and applying average dwell time (ADT) technology.

II. Overall Framework of Asynchronous Switched Event-Triggered LFC Systems

The dynamics of a N-area interconnected LFC system with actuator failures can be described as the following state-space equations [11]:

$$\begin{cases}\dot{x}(t) = Ax(t) + BFu(t) + Ew(t)\\ y(t) = Cx(t)\end{cases} \tag{1}$$

where $x(t) = [x_1^{\mathrm{T}}(t),\ x_2^{\mathrm{T}}(t),\ ...,\ x_N^{\mathrm{T}}(t)]^{\mathrm{T}}$, $x_n(t) = \left[\Delta f_n, \Delta P_{\mathrm{tie}n}, \Delta P_{\mathrm{m}n}, \Delta P_{\mathrm{v}n}, \int ACE_n\right]^{\mathrm{T}}$, $A = [A_{nl}]_{N\times N}$, $B = \mathrm{diag}\{B_n\}$, $E = \mathrm{diag}\{E_n\}$, $C = \mathrm{diag}\{C_n\}$, $u(t) = [u_1(t), u_2(t), ..., u_N(t)]^{\mathrm{T}}$, $F = \mathrm{diag}\{\varphi_n\}$ denotes the fault matrix. A_{nl}, B_n, C_n, E_n are given in [1] , and meanings of notations are demonstrated in Tab. I.

To reduce design conservatism in existing ETC schemes adopting fixed control gains to simultaneously stabilize normal and faulty scenarios, an actuator failure dependent adaptive event-triggered LFC scheme is proposed in this paper. Specifically, the actuator failures in each area are firstly predivided in to Q levels according to the fault severities, i.e., $\varphi_n \overset{\Delta}{=} \{\varphi_{1,n}, \varphi_{2,n}, ..., \varphi_{Q,n}\}$. Therefore, the number of possible operating scenarios of LFC system is N^Q.

TABLE I
Notations In n-th Area

Notations	Explanations
Δf_n	frequency deviation
$\Delta P_{\mathrm{tie}n}$	tie-line power fluctuation
$\Delta P_{\mathrm{m}n}$	mechanical output deviation of generator
$\Delta P_{\mathrm{v}n}$	positional deviation of valve
$\Delta P_{\mathrm{d}N}$	load fluctuation
$ACE_n = \beta_n \Delta f_n + \Delta P_{\mathrm{tie}n}$	Area control error
β_n	frequency bias factor
L_{nl}	tie-line synchronizing coefficient
M_n, D_n	Inertia and damping coefficients of generator
$T_{\mathrm{g}n}, T_{\mathrm{t}n}$	time constants of governor and turbine
R_n	droop coefficient
$\varphi_n \in [0,\ 1]$	actuator failure coefficient
$u_n(t)$	control instruction

Moreover, different from current adaptive triggered threshold update mechanism [9]- [10] without upper bound restrictions, to guarantee monitoring sensitivity and control performance when the state deviations are well damped, the control instruction and ETD adopting bounded adaptive triggered threshold update mechanism under q-th ($q \in \{1, 2, ..., N^Q\}$) faulty scenario are presented as follows.

$$u(t) = K_q x(t_k h), t \in [t_k h + \tau_{t_k}, t_{k+1}h + \tau_{t_{k+1}}) \tag{2}$$

$$t_{k+1}h = t_k h + \min_{l\in N}\left\{ lh \;\middle|\; \begin{array}{l} e^{\mathrm{T}}(i_k h)\Phi_q e(i_k h) \geq \\ \delta_q(t_k h)x^{\mathrm{T}}(t_k h)\Xi_q x(t_k h) \\ \text{or } Q(i_k h) \neq Q(t_k h)\end{array}\right\} \tag{3}$$

where K_q is controller gain, h is sampling time, $t_k h$ ($t_k \in \mathbf{N}$) is triggered instant, τ_{t_k} and $\tau_{t_{k+1}}$ is transmission delays of two neighbouring triggered instants, $i_k h = t_k h + lh$, $Q(i_k h)$ takes values from $\{1, 2, ..., N^Q\}$, $\Phi_q, \Xi_q > 0$ are weighting matrices, $\delta_q(t_k h)$ is the triggered threshold which adopts the following bounded update mechanism.

$$\delta_q(t_k h) = \min\{\overline{\delta}_q, \max\{\underline{\delta}_q, \varepsilon\delta_q(t_{k-1}h)\}\} \tag{4}$$

where $\varepsilon = \begin{cases}0, \Delta y(t_k h) > 0\\ 1-\frac{2\alpha}{\pi}\arctan(\Delta y(t_k h)), \text{otherwise}\end{cases}$, $\Delta y(t_k h) = \frac{||y(t_k h)||_2 - ||y(t_{k-1}h)||_2}{||y(t_{k-1}h)||_2}$, $0 \leq \underline{\delta}_q \leq \overline{\delta}_q < 1$, $\alpha > 1$. Obviously, $\underline{\delta}_q \leq \delta_q(t_k h) \leq \overline{\delta}_q$. Therefore, the asynchronous switched event-triggered LFC scheme contains two parts:

(1) *ETC parameter library*: each option in the library contains two modules, i.e., controller and ETD. Note that there inevitably exists a duration that the ETC parameters do not match the current faulty operating status during parameter adjustment process.

(2) *Update judgement module*: Even each option in ETC parameter library can stabilize the corresponding faulty scenario, too frequent switches among different faulty scenarios may also drive the state trajectories to be divergent. In other words, the proposed ETC scheme require that the LFC system under a specific faulty scenario should continuously operate for a certain time which is called as the dwell time [13].

III. Asynchronous Update Process

The dynamics of the event-triggered LFC system under q-th faulty scenario between two neighbouring triggered instants can be described as follows [8], i.e.,

$$\begin{cases}\dot{x}(t)=Ax(t)+BF_qK_q(x(t-\eta(t))-e(i_kh))+Ew(t)\\ y(t)=Cx(t)\end{cases} \quad (5)$$

where $\eta(t)=t-i_kh$ satisfying $0\leq\eta(t)\leq h+\max\{\tau_{i_k}\}=\bar{\tau}$, τ_{i_k} is the transmission delay at $t=i_kh$, $i_k=t_k, t_k+1, ..., t_{k+1}$. However, the controller and ETD cannot be adjusted synchronously since they are located on the opposite sides of communication network. Therefore, in this section, the asynchronous update process of ETC parameters are discussed. Without loss of generality, the following assumptions are firstly introduced:

- The initial faulty scenario is $q_1\in\{1, 2, ..., N^Q\}$. The faulty operation scenarios will switch to $q_2(\neq q_1)$ at $t=T_1$ and then revert to q_1 at $t=T_2$.
- There exist a definite upper bound of uplink delay (denoted as $\Delta\tau_{\mathrm{u}}$) and downlink delay (denoted as $\Delta\tau_{\mathrm{d}}$), i.e., $\{\Delta\tau_{\mathrm{u}}, \Delta\tau_{\mathrm{d}}\} \leq \max\{\tau_{i_k}\} \triangleq \tau_{\max}$.

There are three stages during ETC parameter update process.

Stage 1 (Failure Reporting): During the time interval $t\in[T_1, T_1+\Delta\tau_{\mathrm{u}})$, the control center has not received the faulty report yet. Therefore, although the actual operating scenario of LFC system has switched from q_1 into q_2, the controller and ETD still adopt the parameters corresponding to the q_1-th scenario and remain unchanged. The closed-loop dynamics of LFC system during $t \in [T_1, T_1 + \Delta\tau_{\mathrm{u}})$ can be described as

$$\dot{x}(t) = Ax(t)+BF_{q_2}K_{q_1}(x(t-\eta(t))-e(i_kh))+Ew(t) \quad (6)$$

The event-triggered communication scheme is given by

$$t_{k+1}h = t_kh + \min_{l\in N}\left\{lh \,\middle|\, \begin{array}{l} e^{\mathrm{T}}(i_kh)\Phi_{q_1}e(i_kh) \geq \\ \delta_{q_1}(t_kh)x^{\mathrm{T}}(t_kh)\Xi_{q_1}x(t_kh)\end{array}\right\} \quad (7)$$

Stage 2 (Asynchronous updating): Once the control center receives the faulty reports at $t = T_1 + \Delta\tau_{\mathrm{u}}$, the controller gain will be immediately adjusted according to the current failure scenario while the corresponding ETD parameters will be sent out at the same time. Note that during $t \in [T_1 + \Delta\tau_{\mathrm{u}}, T_1 + \Delta\tau_{\mathrm{u}} + \tau_{\mathrm{d}})$, the ETD parameters matching current failure scenario have not arrived at the generator side, the closed-loop dynamics and event-triggered communication scheme are described by

$$\dot{x}(t) = Ax(t)+BF_{q_2}K_{q_2}(x(t-\eta(t))-e(i_kh))+Ew(t) \quad (8)$$

$$t_{k+1}h = t_kh + \min_{l\in N}\left\{lh \,\middle|\, \begin{array}{l} e^{\mathrm{T}}(i_kh)\Phi_{q_1}e(i_kh) \geq \\ \delta_{q_1}(t_kh)x^{\mathrm{T}}(t_kh)\Xi_{q_1}x(t_kh)\end{array}\right\} \quad (9)$$

Stage 3 (Synchronous working): Since the ETD parameters have arrived at the generator side after $t = T_1+\Delta\tau_{\mathrm{u}}+\Delta\tau_{\mathrm{d}}$, both the controller and ETD have matched with the current operating scenario. The corresponding closed-loop dynamics can be described by (8) and event-triggered communication scheme are given by

$$t_{k+1}h = t_kh + \min_{l\in N}\left\{lh \,\middle|\, \begin{array}{l} e^{\mathrm{T}}(i_kh)\Phi_{q_2}e(i_kh) \geq \\ \delta_{q_2}(t_kh)x^{\mathrm{T}}(t_kh)\Xi_{q_2}x(t_kh)\end{array}\right\} \quad (10)$$

IV. Design Constraints and Update Criteria

In this section, design constraints and update criteria of our proposed ETC scheme are strictly presented by constructing the Lyapunov functions and adopting ADT technology.

A. Design Constraints of ETC Parameters

The sufficient stability conditions when the faulty scenario switches from q_1 to q_2 are firstly derived.

Based on the Lyapunov stability technique [8], the following theorem can be obtained.

Theorem 1 (*Stability conditions in single faulty switching case*): Given scalars $\sigma, \gamma, \rho_{j,q_2} > 0$ $(j = 1, 2, 3)$, if there exist matrices $K_{q_1}, K_{q_2}, X_{j,q_2}$ and positive symmetric positive definite matrices P, Q_{q_2}, W_{q_2}, R_{q_2} making matrix inequalities (11) and (12) hold, the LFC system is exponentially stable when the faulty scenario switches from q_1 to q_2.

$$\begin{bmatrix} W_{j,q_2} & X_{j,q_2} \\ X_{j,q_2}^{\mathrm{T}} & W_{j,q_2}\end{bmatrix} > 0 \quad (11)$$

$$\begin{bmatrix} \Omega_{j,11} & \Omega_{j,12} & \Omega_{j,13} & \Omega_{j,14} & \Omega_{j,15} & \Omega_{j,16} & \Omega_{j,17} \\ * & \Omega_{j,22} & \Omega_{j,23} & 0 & 0 & 0 & 0 \\ * & * & \Omega_{j,33} & \Omega_{j,34} & 0 & \Omega_{j,36} & 0 \\ * & * & * & \Omega_{j,44} & 0 & \Omega_{j,46} & 0 \\ * & * & * & * & \Omega_{j,55} & \Omega_{j,56} & 0 \\ * & * & * & * & * & \Omega_{j,66} & 0 \\ * & * & * & * & * & * & \Omega_{j,77}\end{bmatrix} < 0 \quad (12)$$

where $\Omega_{1,11} = \Omega_{2,11} = -\sigma P+A^{\mathrm{T}}P+PA+Q_{q_2}-\varphi W_{q_2}-\frac{\pi^2}{4}R_{q_2}$, $\Omega_{3,11} = \lambda P+A^{\mathrm{T}}P+PA+Q_{q_2}-\psi W_{q_2}-\frac{\pi^2}{4}R_{q_2}$, $\Omega_{1,12} = \varphi X_{1,q_2}^{\mathrm{T}}$, $\Omega_{2,12} = \varphi X_{2,q_2}^{\mathrm{T}}$, $\Omega_{3,12} = \psi X_{3,q_2}^{\mathrm{T}}$, $\Omega_{1,13} = PBF_{q_2}K_{q_1} - \varphi\left(X_{1,q_2}^{\mathrm{T}}-W_{q_2}\right) + \frac{\pi^2}{4}R_{q_2}$, $\Omega_{2,13} = PBF_{q_2}K_{q_2}-\varphi\left(X_{2,q_2}^{\mathrm{T}}-W_{q_2}\right)+\frac{\pi^2}{4}R_{q_2}$, $\Omega_{3,13}=PBF_{p_2}K_{q_2}-\psi\left(X_{3,q_2}^{\mathrm{T}}-W_{q_2}\right)+\frac{\pi^2}{4}R_{q_2}$, $\Omega_{1,14} = -PBF_{q_2}K_{q_1}$, $\Omega_{2,14} = \Omega_{3,14} = -PBF_{q_2}K_{q_2}$, $\Omega_{1,15} = \Omega_{2,15} = \Omega_{3,15} = {\Omega_{j,56}}^{\mathrm{T}} = PE$, $\Omega_{1,16} = \Omega_{2,16} = \Omega_{3,16} = A^{\mathrm{T}}P$, $\Omega_{1,17} = \Omega_{2,17} = \Omega_{3,17} = C^{\mathrm{T}}$, $\Omega_{1,22} = \Omega_{2,22} = -e^{\sigma\bar{\tau}}Q_{q_2} - \varphi W_{q_2}$, $\Omega_{3,22} = -e^{-\lambda\bar{\tau}}Q_{q_2} - \psi W_{q_2}$, $\Omega_{1,23} = -\varphi\left(-W_{q_2}+X_{1,q_2}\right)$, $\Omega_{2,23} = -\varphi\left(-W_{q_2}+X_{2,q_2}\right)$, $\Omega_{3,23} = -\psi\left(-W_{q_2}+X_{3,q_2}\right)$, $\Omega_{1,33} = -\varphi\left(2W_{q_2}-X_{1,q_2}^{\mathrm{T}}-X_{1,q_2}\right)-\frac{\pi^2}{4}R_{q_2}+\bar{\delta}_{q_1}\Xi_{q_1}$, $\Omega_{2,33}=-\varphi\left(2W_{q_2}-X_{2,q_2}^{\mathrm{T}}-X_{2,q_2}\right)-\frac{\pi^2}{4}R_{q_2}+\bar{\delta}_{q_1}\Xi_{q_1}$, $\Omega_{3,33}=-\psi\left(2W_{q_2}-X_{3,q_2}^{\mathrm{T}}-X_{3,q_2}\right)-\frac{\pi^2}{4}R_{q_2}+\bar{\delta}_{q_2}\Xi_{q_2}$, $\Omega_{1,34} = \Omega_{2,34} = -\bar{\delta}_{q_1}\Xi_{q_1}$, $\Omega_{3,34} = -\bar{\delta}_{q_2}\Xi_{q_2}$, $\Omega_{1,36} = -\Omega_{1,36} = {K_{q_1}}^{\mathrm{T}}{F_{q_2}}^{\mathrm{T}}B^{\mathrm{T}}P$, $\Omega_{2,36} = \Omega_{3,36} = -\Omega_{2,46} = -\Omega_{3,46} = {K_{q_2}}^{\mathrm{T}}{F_{q_2}}^{\mathrm{T}}B^{\mathrm{T}}P$, $\Omega_{1,44} = \Omega_{2,44} = \bar{\delta}_{q_1}\Xi_{q_1}-\Phi_{q_1}$, $\Omega_{3,44}=\bar{\delta}_{q_2}\Xi_{q_2}-\Phi_{q_2}$, $\Omega_{j,55}=-\gamma^2 I$, $\Omega_{j,66}={\rho_{j,q_2}}^2(\bar{\tau}^2W_{q_2}+\bar{\tau}^2R_{q_2})-2\rho_{j,q_2}P$, $\Omega_{j,77}=-I$, $\varphi=\frac{-\sigma\bar{\tau}}{e^{-\sigma\bar{\tau}}-1}$, $\psi=\frac{\lambda\bar{\tau}}{e^{\lambda\bar{\tau}}-1}$.

To address the nonlinear terms in (13), let $\Lambda = P^{-1}$, $Y_{q_1} = K_{q_1}\Lambda$, $Y_{q_2} = K_{q_2}\Lambda$, $\tilde{Q}_{q_2} = \Lambda Q_{q_2}\Lambda$, $\tilde{W}_{q_2} = \Lambda W_{q_2}\Lambda$, $\tilde{R}_{q_2} = \Lambda R_{q_2}\Lambda$, $\tilde{X}_{j,q_2} = \Lambda X_{j,q_2}\Lambda$, $\tilde{\Xi}_{q_1} = \Lambda\Xi_{q_1}\Lambda$, $\tilde{\Xi}_{q_2} = \Lambda\Xi_{q_2}\Lambda$, $\tilde{\Phi}_{q_1} = \Lambda\Phi_{q_1}\Lambda$, $\tilde{\Phi}_{q_2} = \Lambda\Phi_{q_2}\Lambda$. By pre- and post-multiply both sides of (12) and (13) with $diag\{\Lambda, \Lambda\}$ and $diag\{\Lambda, \Lambda, \Lambda, \Lambda, I, \Lambda, I, I, I\}$ respectively, the following equivalent corollary can be obtained.

Corollary 1 (*Parameter design constraints*): Given scalars $\sigma, \gamma, \rho_{j,q_2} > 0$ $(j = 1, 2, 3)$, if there exist matrices Y_{q_1}, Y_{q_2}, $\tilde{X}_{j,q_2}$ and positive symmetric positive definite matrices Λ, $\tilde{Q}_{q_2}$, $\tilde{W}_{q_2}$, $\tilde{R}_{q_2}$ making (13) and (14) hold, the LFC system is exponentially stable when failure scenario switches from q_1 to q_2. The controller gains and weighting matrices satisfy $K_{q_1} = Y_{q_1}\Lambda^{-1}$, $K_{q_2} = Y_{q_2}\Lambda^{-1}$, $\Phi_{q_1} = \Lambda^{-1}\tilde{\Phi}_{q_1}\Lambda^{-1}$, $\Phi_{q_2}=\Lambda^{-1}\tilde{\Phi}_{q_2}\Lambda^{-1}$, $\Xi_{q_1}=\Lambda^{-1}\tilde{\Xi}_{q_1}\Lambda^{-1}$, $\Xi_{q_2}=\Lambda^{-1}\tilde{\Xi}_{q_2}\Lambda^{-1}$.

$$\begin{bmatrix} \tilde{W}_{j,q_2} & \tilde{X}_{j,q_2} \\ \tilde{X}^T_{j,q_2} & \tilde{W}_{j,q_2} \end{bmatrix} > 0 \quad (13)$$

$$\begin{bmatrix} \tilde{\Omega}_{j,11} & \tilde{\Omega}_{j,12} & \tilde{\Omega}_{j,13} & \tilde{\Omega}_{j,14} & \tilde{\Omega}_{j,15} & \tilde{\Omega}_{j,16} & \tilde{\Omega}_{j,17} \\ * & \tilde{\Omega}_{j,22} & \tilde{\Omega}_{j,23} & 0 & 0 & 0 & 0 \\ * & * & \tilde{\Omega}_{j,33} & \tilde{\Omega}_{j,34} & 0 & \tilde{\Omega}_{j,36} & 0 \\ * & * & * & \tilde{\Omega}_{j,44} & 0 & \tilde{\Omega}_{j,46} & 0 \\ * & * & * & * & \tilde{\Omega}_{j,55} & \tilde{\Omega}_{j,56} & 0 \\ * & * & * & * & * & \tilde{\Omega}_{j,66} & 0 \\ * & * & * & * & * & * & \tilde{\Omega}_{j,77} \end{bmatrix} < 0 \quad (14)$$

where $\tilde{\Omega}_{1,11}=\tilde{\Omega}_{2,11}=-\sigma\Lambda+\Lambda A^{\mathrm{T}}+A\Lambda+\tilde{Q}_{q_2}-\varphi\tilde{W}_{q_2}-\frac{\pi^2}{4}\tilde{R}_{q_2}$, $\tilde{\Omega}_{3,11}=\lambda\Lambda+\Lambda A^{\mathrm{T}}+A\Lambda+\tilde{Q}_{q_2}-\psi\tilde{W}_{q_2}-\frac{\pi^2}{4}\tilde{R}_{q_2}$, $\tilde{\Omega}_{1,12}=\varphi\tilde{X}^{\mathrm{T}}_{1,q_2}$, $\tilde{\Omega}_{2,12}=\varphi\tilde{X}^{\mathrm{T}}_{2,q_2}$, $\tilde{\Omega}_{3,12}=\psi\tilde{X}^{\mathrm{T}}_{3,q_2}$, $\tilde{\Omega}_{1,13}=BF_{q_2}Y_{q_1}-\tilde{\varphi}(X^{\mathrm{T}}_{1,q_2}-\tilde{W}_{q_2})+\frac{\pi^2}{4}\tilde{R}_{q_2}$, $\tilde{\Omega}_{2,13}=BF_{q_2}Y_{q_2}-\varphi(\tilde{X}^{\mathrm{T}}_{2,q_2}-\tilde{W}_{q_2})+\frac{\pi^2}{4}\tilde{R}_{q_2}$, $\tilde{\Omega}_{3,13}=BF_{q_2}Y_{q_1}-\psi(\tilde{X}^{\mathrm{T}}_{3,q_2}-\tilde{W}_{q_2})+\frac{\pi^2}{4}\tilde{R}_{q_2}$, $\tilde{\Omega}_{1,14}=-BF_{q_2}Y_{q_1}$, $\tilde{\Omega}_{2,14}=\tilde{\Omega}_{3,14}=-BF_{q_2}Y_{q_2}$, $\tilde{\Omega}_{1,15}=\tilde{\Omega}_{2,15}=\tilde{\Omega}_{3,15}=\tilde{\Omega}^{\mathrm{T}}_{j,56}=E$, $\tilde{\Omega}_{1,16}=\tilde{\Omega}_{2,16}=\tilde{\Omega}_{3,16}=\Lambda A^{\mathrm{T}}$, $\tilde{\Omega}_{1,17}=\tilde{\Omega}_{2,17}=\tilde{\Omega}_{3,17}=\Lambda C^{\mathrm{T}}$, $\tilde{\Omega}_{1,22}=\tilde{\Omega}_{2,22}=-e^{\sigma\bar{\tau}}\tilde{Q}_{q_2}-\varphi\tilde{W}_{q_2}$, $\tilde{\Omega}_{3,22}=-e^{-\lambda\bar{\tau}}\tilde{Q}_{q_2}-\psi\tilde{W}_{q_2}$, $\tilde{\Omega}_{3,22}=-e^{-\lambda\bar{\tau}}\tilde{Q}_{q_2}-\psi\tilde{W}_{q_2}$, $\tilde{\Omega}_{1,23}=\varphi(\tilde{W}_{q_2}-\tilde{X}_{1,q_2})$, $\tilde{\Omega}_{2,23}=\varphi(\tilde{W}_{q_2}-\tilde{X}_{2,q_2})$, $\tilde{\Omega}_{3,23}=\psi(\tilde{W}_{q_2}-\tilde{X}_{3,q_2})$, $\tilde{\Omega}_{1,33}=\varphi(-2\tilde{W}_{q_2}+\tilde{X}^{\mathrm{T}}_{1,q_2}+\tilde{X}_{1,q_2})-\frac{\pi^2}{4}\tilde{R}_{q_2}+\bar{\delta}_{p_1}\tilde{\Xi}_{q_1}$, $\tilde{\Omega}_{2,33}=\varphi(-2\tilde{W}_{q_2}+\tilde{X}^{\mathrm{T}}_{1,p_2}+\tilde{X}_{1,q_2})-\frac{\pi^2}{4}\tilde{R}_{q_2}+\bar{\delta}_{q_1}\tilde{\Xi}_{q_1}$, $\tilde{\Omega}_{3,33}=\psi(-2\tilde{W}_{q_2}+\tilde{X}^{\mathrm{T}}_{1,q_2}+\tilde{X}_{1,q_2})-\frac{\pi^2}{4}\tilde{R}_{q_2}+\bar{\delta}_{q_2}\tilde{\Xi}_{q_2}$, $\tilde{\Omega}_{1,34}=\tilde{\Omega}_{2,34}=-\bar{\delta}_{q_1}\tilde{\Xi}_{q_1}$, $\tilde{\Omega}_{3,34}=-\bar{\delta}_{q_2}\tilde{\Xi}_{q_2}$, $\tilde{\Omega}_{1,36}=-\tilde{\Omega}_{1,36}=Y_{q_1}^{\mathrm{T}}F_{q_2}^{\mathrm{T}}B^{\mathrm{T}}$, $\Omega_{2,36}=\Omega_{3,36}=-\Omega_{2,46}=-\Omega_{3,46}=Y_{q_2}^{\mathrm{T}}F_{q_2}^{\mathrm{T}}B^{\mathrm{T}}$, $\tilde{\Omega}_{1,44}=\tilde{\Omega}_{2,44}=\bar{\delta}_{q_1}\tilde{\Xi}_{q_1}-\tilde{\Phi}_{q_1}$, $\tilde{\Omega}_{3,44}=\bar{\delta}_{q_2}\tilde{\Xi}_{q_2}-\tilde{\Phi}_{q_2}$, $\tilde{\Omega}_{j,55}=-\gamma^2 I$, $\tilde{\Omega}_{j,66}=\rho^2_{j,q_2}\bar{\tau}^2(\tilde{W}_{q_2}+\tilde{R}_{q_2})-2\rho_{j,q_2}\Lambda$, $\tilde{\Omega}_{j,77}=-I$.

B. Update Criteria Under Stochastic Failure Switching Cases

Theorem 1 and Corollary 1 can only guarantee the closed-loop stability under single failure switching cases. However, it must be pointed out that short-term stochastic fault changes can still drive the state trajectories of LFC system to be divergent. As aforementioned, the proposed scheme requires that the LFC system should operate under a certain faulty scenario for a period of time. In this subsection, the update criteria of ETC parameters in arbitrary two fault switching case are derived with the average dwell time (ADT) technology. The following theorem is presented.

Based on the average dwell time technique [12], the following theorem can be obtained.

Theorem 2 (*Update criteria of ETC parameters*): Given scalars $\sigma, \gamma, \rho_{j,q_2} > 0$ $(j=1,2,3)$, if there exist a scalar $\mu > 1$, matrices $K_{q_1}, K_{q_2}, X_{j,q_1}, X_{j,q_2}$ and symmetric positive definite matrices $P, Q_{q_1}, Q_{q_2}, W_{q_1}, W_{q_2}, R_{q_1}, R_{q_2}$ satisfying matrix inequalities (11) and (12) and inequalities (15)-(17), the LFC system is H_∞ exponentially stable when randomly switching between faulty scenarios q_1 and q_2.

$$Q_{q_1} \le \mu Q_{q_2}, W_{q_1} \le \mu W_{q_2}, R_{q_1} \le \mu R_{q_2} \quad (15)$$

$$Q_{q_2} \le \mu Q_{q_1}, W_{q_2} \le \mu W_{q_1}, R_{q_2} \le \mu R_{q_1} \quad (16)$$

$$T_{\mathrm{d}q_1,q_2} \ge \frac{\ln\mu + (\sigma+\lambda)\times(3\bar{\tau})}{\lambda} \triangleq \bar{T}_{\mathrm{d}q_1,q_2} \quad (17)$$

where $\bar{T}_{\mathrm{d}q_1,q_2}$ is the required minimal ADT.

TABLE II
SIMULATION PARAMETERS OF TWO-AREA POWER SYSTEM

Areas	T_{ti}/s	T_{gi}/s	R_i/Hz·p.u.$^{-1}$	β_i/p.u.·s	D_i/p.u.·s	M_i/p.u.·s^2
1	0.3	0.1	0.05	21.0	1.0	10
2	0.3	0.1	0.05	21.5	1.5	12
$T_{12}=T_{21}=0.1986$ p.u. · rad^{-1}						

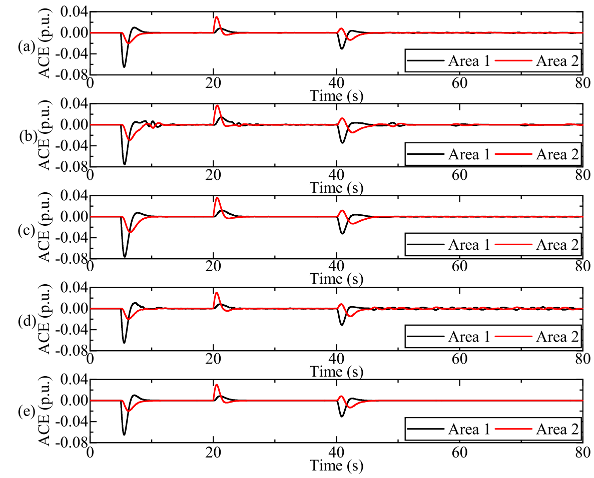

Fig. 1. ACE responses with different control schemes(single fault switching scenario): (a) This paper; (b) UAETC without considering fault [9]; (c) FETC considering faults [11]; (d) Asynchronous switched UAETC; (e) Asynchronous switched PTC [12].

V. CASE STUDIES AND DISCUSSIONS

In this section, a two-area LFC system is simulated and discussed to verify the effectiveness of our proposed asynchronous switched ETC scheme. Simulation parameters are demonstrated in Tab.II. The following schemes are chose as comparisons: (1) Unbounded adaptive ETC scheme without considering actuator faults (UAETC) [9]; (2) Fixed-thershold ETC scheme [11]; (3) Asynchronous switched UAETC scheme; and (4) Asynchronous periodic triggered control (PTC) scheme [12].

Without loss of generality, we set the following two faulty scenarios as F_1=diag$\{\varphi_{1,1},\varphi_{1,2}\}$=diag$\{0.75,0.75\}$ (Scenario 1) and F_2=diag$\{\varphi_{2,1},\varphi_{2,2}\}$=diag$\{0.25,0.25\}$ (Scenario 2). Moreover, let $\tau_{\max}$=10ms, h=10ms, σ=1.1, λ=1.5, α=1.2, $\underline{\delta}_1$=$\underline{\delta}_2$=0.0001, $\bar{\delta}_1$=$\bar{\delta}_2$=0.05, γ=7.5, $\rho_{j,1}$=$\rho_{j,2}$=4.25. The required minimal ADT of our proposed asynchronous switched ETC scheme is $\overline{T}_{\mathrm{d}1,2}=3.08$s.

Assume that the LFC system initially operates under Scenario 1 and then switches to Scenario 2 at t=40s. In addition, suppose that two step external power disturbances occur in Area 1 (at $t=5$s) and Area 2 (at $t=20$s), respectively. The corresponding amplitudes are 0.1 p.u. and -0.15 p.u., respectively. Fig. 1 shows the ACE responses with different control schemes. Fig. 2 presents the triggered intervals of different ETC schemes. Moreover, the triggered time and average value of integral of absolute error (IAE$_{\mathrm{av}}$) with each scheme are demonstrated in Fig. 3.

It can be seen that the lowest IAE$_{\mathrm{av}}$ of ACE responses in two area can be guaranteed with adopting the asynchronous PTC scheme [12] since the operation statues are always moni-

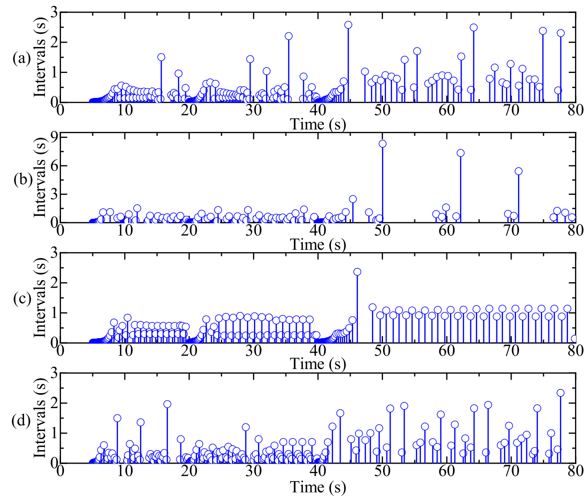

Fig. 2. Triggered intervals with different ETC schemes (single fault switching scenario): (a) This paper; (b) UAETC without considering fault [9]; (c) FETC considering faults [11]; (d) Asynchronous switched UAETC [12].

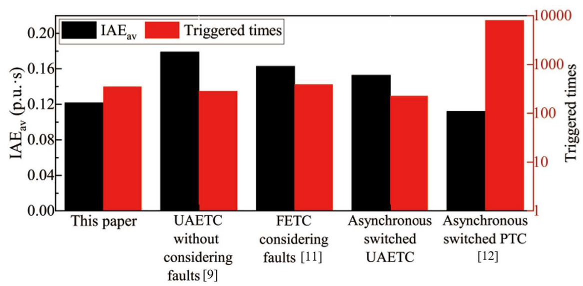

Fig. 3. Control performance under single fault switching scenarios.

tored at each sampled instant. In [9], the actuator failures have not been considered in ETC parameter design process and the update ranges have not been restricted. Therefore, the average IAE of ACE responses with the control scheme proposed in [9] is 47.0% larger compared with our proposed method. Different from the fixed-gain ETC schemes [11] taking the actuator failures into account, a series of ETC parameters are designed in this paper to stabilize the preset operation scenario with different failure severities. Therefore, the design conservatism can be reduced. Moreover, in this paper, the triggered threshold can be adaptively improved with the decrease of ACE responses, the $\mathrm{IAE}_{\mathrm{av}}$ of ACE and triggered times can be reduced by 25.20% and 10.26% respectively compared with [11]. For the unbounded adaptive update mechanism, the triggered threshold will be quickly increased when the ACEs start to be damped. As a consequence, more larger deviations of ACE responses are required to trigger the operation state upload and control instruction update. Conversely, in our proposed scheme, the threshold value is strictly limited within a specific range to guarantee a sensitive operation status perception ability of LFC system. Therefore, although the triggered times with our proposed method are 123 larger compared with the asynchronous UAETC scheme, the average IAE of ACE responses can be reduced by 20.30%. In short, the proposed asynchronous switched ETC scheme have a better transient damping performance than other ETC schemes in presence of the external power disturbances. Finally, considering that over 95.6% of triggered times is reduced by adopting our proposed ETC scheme compared with the PTC scheme, the operation resilience under limited network resources can be effectively enhanced.

VI. Conclusion

To enhance the frequency stability of multi-area power systems in presence of stochastic actuator failures, in this paper, an asynchronous switched event-triggered LFC scheme has been proposed. A series of operating scenarios representing different actuator failure severities have been firstly preset. Moreover, the ETC parameter options corresponding to the preset failure scenarios have been designed for potential actuator failures. Fully considering that the ETC parameters do not match the actual operating scenario during the control parameter adjustment process, the ETC parameter design constraints and update criteria have been strictly derived. The simulation results show that the LFC system with our proposed method has good operational resilience in the face of stochastic actuator failures. In the future, further efforts will be paid on the design of asynchronous switched event-triggered LFC under cyber attacks.

References

[1] C.-H. Yan, B. Liu, P. Xiao, and C. Zhang, "Stabilization of load frequency control system via event-triggered intermittent control," *IEEE Trans. Circuits-II*, vol. 69, no. 12, pp. 4934–4938, 2022.

[2] S. Kuppusamy, Y. H. YJoo, and H. Sol Kim, "Fault-tolerant load frequency control for dfig-based interconnected wind power systems," *Inform. Sciences*, vol. 582, pp. 73–88, 2022.

[3] X. Su, X. Liu, and Y.-D. Song, "Fault-tolerant control of multiarea power systems via a sliding-mode observer technique," *IEEE-ASME Trans. Mech.*, vol. 23, no. 1, pp. 38–47, 2018.

[4] Y. Zhang, C. Peng, S. Xie, and X. Du, "Deterministic network calculus-based h_∞ load frequency control of multiarea power systems under malicious dos attacks," *IEEE Trans. Smart Grid*, vol. 13, no. 2, pp. 1542–1554, 2022.

[5] H. Luo and Z. Hu, "Stability analysis of sampled-data load frequency control systems with multiple delays," *IEEE Trans. Contr. Syst. T.*, vol. 30, no. 1, pp. 434–442, 2022.

[6] P. Oziablo, D. Mozyrska, and M. Wyrwas, "Fractional-variable-order digital controller design tuned with the chaotic yellow saddle goatfish algorithm for the avr system," *ISA Trans.*, vol. 125, pp. 260–267, 2022.

[7] C.-H. Yan, B. Liu, P. Xiao, and C. Zhang, "Stabilization of load frequency control system via event-triggered intermittent control," *IEEE Trans. Circuits-II*, vol. 69, no. 12, pp. 4934–4938, 2022.

[8] C. Peng and T. C. Yang, "Event-triggered communication and h_∞ control co-design for networked control systems," *Automatica*, vol. 49, no. 5, pp. 1326–1332, 2013.

[9] C. Peng, J. Zhang, and H. Yan, "Adaptive event-triggering H_∞ load frequency control for network-based power systems," *IEEE Trans. Ind. Electron.*, vol. 65, no. 2, pp. 1685–1694, 2018.

[10] H. Zhang, J. Liu, and S. Xu, "H-infinity load frequency control of networked power systems via an event-triggered scheme," *IEEE Trans. Ind. Electron.*, vol. 67, no. 8, pp. 7104–7113, 2020.

[11] H. Shen, Y. Xia, J. Wang, and J. H. Park, "Fault-tolerant event-triggered $\mathcal{H}_\infty$ load frequency control for multiarea power systems with communication delay," *IEEE Syst. J.*, vol. 16, no. 4, pp. 6624–6634, 2022.

[12] L. Zhang and H. Gao, "Asynchronously switched control of switched linear systems with average dwell time," *Automatica*, vol. 46, no. 5, pp. 953–958, 2010.

[13] Y. Zhang, C. Peng, C. Cheng, and Y.-L. Wang, "Attack intensity dependent adaptive load frequency control of interconnected power systems under malicious traffic attacks," *IEEE Trans. Smart Grid*, vol. 14, no. 2, pp. 1223–1235, 2023.